Zirconium-Polycarboxylato Gel Systems as Substrate to Develop Advanced Fluorescence Sensing Devices

Jon Pascual-Colino *, Garikoitz Beobide, Oscar Castillo *, Javier Cepeda, Mónica Lanchas, Antonio Luque, Sonia Pérez-Yáñez

Posted Date: 7 November 2024

doi: 10.20944/preprints202411.0531.v1

Keywords: zirconium; metal-organic gels; fluorescence; chemical-sensor

Article

Zirconium-Polycarboxylato Gel Systems as Substrate to Develop Advanced Fluorescence Sensing Devices

Jon Pascual-Colino [1,2,*], Garikoitz Beobide [1,2], Oscar Castillo [1,2,*], Javier Cepeda [3], Mónica Lanchas [4], Antonio Luque [1,2] and Sonia Pérez-Yáñez [1,2]

[1] Departamento de Química Orgánica e Inorgánica, Facultad de Ciencia y Tecnología, Universidad del País Vasco, UPV/EHU, Apartado 644, E-48080 Bilbao, Spain
[2] BCMaterials, Basque Center for Materials, Applications and Nanostructures, UPV/EHU Science Park, E-48940 Leioa, Spain;
[3] Departamento de Química Aplicada, Facultad de Química, Universidad del País Vasco, UPV/EHU, 20018 Donostia-San Sebastián, Spain
[4] Departamento de Ingeniería Química, Facultad de Ciencia y Tecnología, Universidad del País Vasco, UPV/EHU, Apartado 644, E-48080 Bilbao, Spain
* Correspondence: jon.pascual@ehu.eus (J.P.-C.); oscar.castillo@ehu.eus (O.C.)

Abstract: This study presents the development of zirconium polycarboxylate gel systems as substrates for advanced fluorescence sensing devices. Zirconium-based metal-organic gels (MOGs) offer a promising alternative due to the robustness of the Zr–O bond, which provides enhanced chemical stability. In this work, zirconium polycarboxylate gels were synthesized using green solvents in a rapid room temperature method. Fluorescein, naphthalene-2,6-dicarboxylic acid and 4,4',4'',4'''-(porphine-5,10,15,20-tetrayl)tetrakisbenzoic acid were incorporated as fluorophores to give the gel luminescent properties, enabling it to be used as a sensor. These fluorophores produce specific changes in the perceived colour and intensity of the fluorescence emission upon interaction with different analytes in solution, allowing a qualitative identification of different solvents and compounds. However, the fragile structure of neat gels hinders reproducible quantitative analysis of fluorescence emission, so to increase mechanical stability during manipulation, a composite material was developed by combining the MOGs with quartz microcrystals, which proved to be a more reliable fluorescent system. The results show that the material can identify univocally different solvents and analytes in aqueous solutions by the quantitative analysis of the emissions intensities. This work presents an innovative approach to create advanced fluorescence sensors with improved mechanical properties and stability using zirconium polycarboxylate gels and multiple fluorophores.

Keywords: zirconium; metal-organic gels; fluorescence; chemical-sensor

1. Introduction

Metal-organic porous materials represent a significant research field in materials science during the last decades, with numerous applications [1]. However, in some cases, their stability is inadequate, and the material cannot withstand the necessary conditions for the application. To enhance the stability of the system, zirconium-based metal-organic materials can be used due to strength of the Zr–O bond [2]. Among them, several porous gels (MOGs, metal-organic gels) have been prepared containing $[Zr_6(O)_4(OH)_4]^{12+}$ clusters connected by polycarboxylato ligands [3,4]. Gels based on Zr(IV) and polycarboxylate ligands [5,6] are complex materials that combine the properties of polymers with the capabilities provided by the presence of the zirconium atoms to generate an uncountable number of applications, such as sensor[7], energy storage[8], gas storage/removal[9], etc.

Most of the MOGs reported are obtained through an energetically demanding route (i.e. employing heating procedures) and with environmentally unsustainable solvents such as N,N-dimethylformamide, N,N-dimethylacetamide or hydrochloric acid. In our research group we have prepared several zirconium based metal-organic gels containing the abovementioned $[Zr_6(O)_4(OH)_4]^{12+}$ SBU and polycarboxylic ligands through a rapid method (1-2 min) at room

 doi:10.20944/preprints202411.0531.v1

temperature, with green solvents and without employing modulators such as HCl and acetic acid [10]. Among them a thermally and chemically robust MOG of general formula $[Zr_6(O)_4(OH)_4(BTC)_{2.13}(HBTC)_{2.81}]\cdot n$ solvent was synthesized, where BTC is the benzene-1,3,5-tricarboxylate anion (trimesate anion). The porosity and features of this material allowed us to use it as a stable catalyst in the continuous electroreduction of CO_2 [10]. Now, the aim of the present work is to take advantage of the characteristics of this material to introduce different molecules with luminescent properties[11] into its structure so that it can be used as a sensor [12,13]. Three fluorophores were selected (Scheme 1): fluorescein (HFL), which contains a single carboxylic group capable of bonding with Zr metal atoms, naphthalene-2,6-dicarboxylic acid (H_2NDC)[14], which has two carboxylic groups, and 4,4',4'',4'''-(porphine-5,10,15,20-tetrayl)tetrakisbenzoic acid (H_4TCPP) [15,16], a molecule with four bridging-capable carboxylic groups. These molecules shows a luminescent response in blue, yellow, and red, respectively, which is retained when anchored to the Zr(IV) metal centers. In principle, these fluorophores, in their anionic form, will replace some of the trimesate anions in the gel. Interestingly, the luminescence emission will undergo significative changes when this functionalized MOG is suspended in different solvents or in aqueous solutions containing different analytes. The change of the luminescent signal of each fluorophore under these conditions can be employed for sensing purposes [17], but these changes are more specific when the three fluorophore molecules are present simultaneously in the MOG. The interaction of the adsorbed molecules modifies to a different extent the luminescent signals of each fluorophore present in the MOG to provide a characteristic colour for each analyte, resulting from the sum of the three emissions. However, the emission intensity is also affected by self-quenching and changes on the fluorophore density can generate significant variations on the emission features that hinder their use as chemical sensors. This fact altogether with the mechanical weakness that these MOGs, and most gels, typically exhibit[18,19] has made necessary to combine the original MOG with mechanically robust quartz microcrystals to form a functional composite sensor [20]. The results will show that the MOG containing the three fluorophores incorporated into a matrix of quartz microcrystals provides the required mechanical strength as to be used to identify different solvents and analytes in aqueous solutions by measuring the relative intensities of the characteristic emission signals of each fluorophore upon UV excitation.

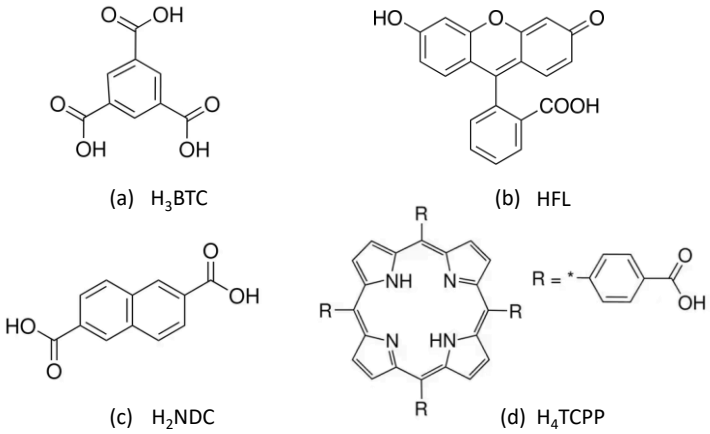

Scheme 1. Bridging ligand and selected fluorophore molecules: (a) benzene-1,3,5-tricarboxylic acid, (b) fluorescein, (c) naphthalene-2,6-dicarboxylic acid and (d) 4,4',4'',4'''-(porphine-5,10,15,20-tetrayl)tetrakisbenzoic acid.

2. Results and Discussion

To develop a fluorescent sensor based on these materials, three fluorophores whose fluorescence emission closely matches the three primary colours (blue, yellow, and red) were selected: naphthalene-2,6-dicarboxylic acid (H_2NDC), fluorescein (HFL) and 4,4',4'',4'''-(porphine-5,10,15,20-tetrayl)tetrakisbenzoic acid (H_4TCPP). Their combination within the same porous matrix provides a material that, upon excitation with the same wavelength, changes the emission of each fluorophore in a non-equal way, resulting in colour changes visible to the naked eye. The fast gelation conditions

 doi:10.20944/preprints202411.0531.v1

obtained under the above-described synthetic conditions facilitates the incorporation of these complex mixtures of fluorophores by the coordination of their deprotonated counterparts to the zirconium metal centers avoiding any possible segregation that could take place under slower thermodynamically driven reaction conditions. As result, this approach provided MOGs with deep blue (421 nm; *Zr-BTC-NDC*), yellow (530 nm; *Zr-BTC-FL*) and red (680/712 nm; *Zr-BTC-TCPP*) emissions (Figure 1 and S5a). It is worth noting that the *Zr-BTC* gel also produces a fluorescence response at the violet spectrum (393 nm) but it is too weak to be used effectively for sensing purposes. The fluorescence maximum of the fluorophores anchored to the Zr-BTC system undergoes a slight redshift compared to the free molecule dissolved in water (380 nm for H_3BTC [21], 426 nm for H_2NDC [22,23], 500 nm for HFL [24], and 643/706 nm for the Q(0,0) and Q(0,1) emissions of H_4TCPP [25–27]).

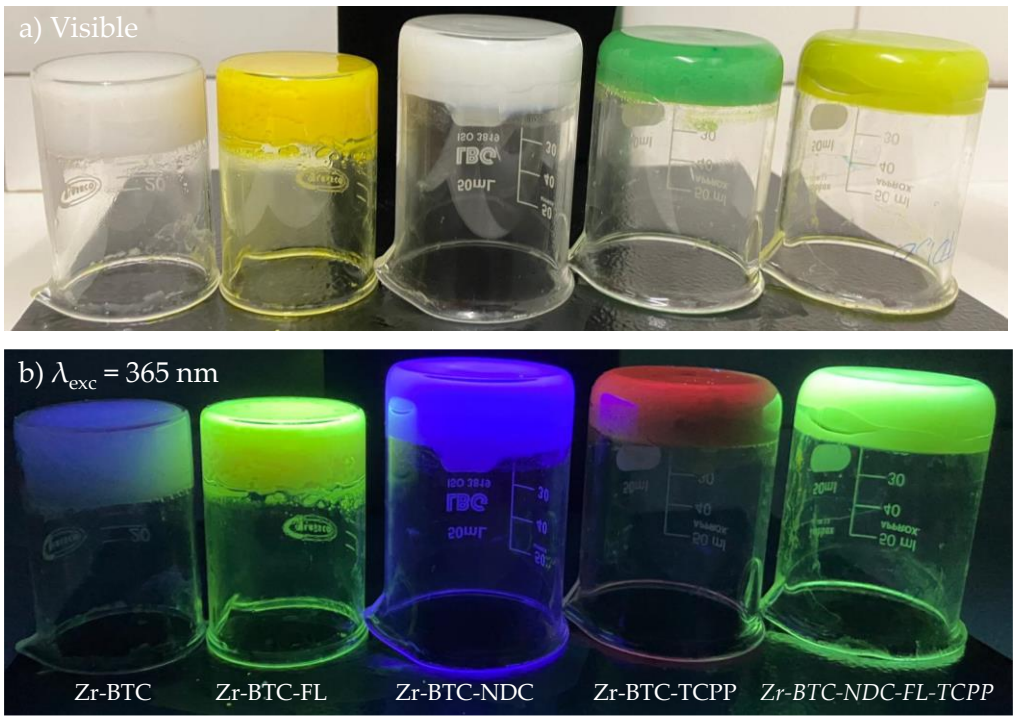

Figure 1. Images of fresh prepared MOGs under visible light (a) and under UV excitation. Note that after washing the gel with methanol during 48h, exchanging the solvent 4 times per day, the luminescence of *Zr-BTC-FL* turned yellow and that of *Zr-BTC-NDC-FL-TCPP* turned more whitish.

Upon exposure of the three fluorophores incorporated *Zr-BTC-NDC-FL-TCPP* gel to different solvents, the visual inspection of the samples reveals changes of the fluorescence emissions (Figure 2a). However, when quantitative measurements are attempted, there is not reproducibility as any manipulation of the gel, as those required to place the sample in the fluorimeter, leads to deformations/densifications of the monolith that also affect the intensity of the fluorescence emissions due to self-quenching effects (Figure S5b). The corresponding aerogel was also prepared by CO_2 supercritical drying, and it retains the fluorescence (Figure 2b) but the resulting monoliths are so fragile that again there is no option to obtain reproducible luminescence measurements.

 doi:10.20944/preprints202411.0531.v1

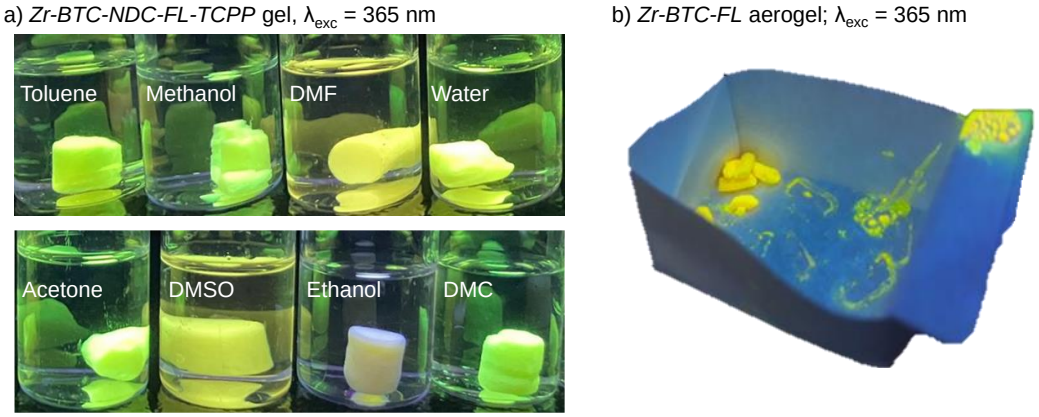

Figure 2. (a) Images of fresh prepared *Zr-BTC-NDC-FL-TCPP* MOGs fluorescence emission under 365 nm excitation when immerse in different solvents. (b) Fluorescence emission under 365 nm excitation of *Zr-BTC-FL* aerogel.

Therefore, an alternative strategy was approached in which, instead of generating macroscopic gel monoliths, nanometric particles of the gel were grown within a matrix of SiO_2 microcrystals intended to protect the fluorescent metal-organic nanoparticles from external mechanical stress. SiO_2 (quartz) was selected because of its transparency towards visible light and a significant portion of UV (> 200 nm). The preparation of this mixture was performed using the same conditions as for metallogels but adding the micrometric quartz particles (90% quartz and 10% metallogel) under vigorous stirring for 12 h. The resulting product was thoroughly washed with methanol using a soxhlet apparatus until the washing liquid remained colourless and did not show any fluorescence emission upon exposure to an UV lamp (365 and 254 nm). Finally, the product was dried at room temperature. SEM/EDX images showed that SiO_2 microcrystals were surrounded by far smaller agglomerates of particles of the *Zr-BTC-NDC-FL-TCPP* gel (Figures 3a, S3 and S4). Under these conditions the fluorescence response remained stable during manipulation, enabling quantitative measurements. The big size difference between the quartz microcrystals and the *MOG* nanoparticles prevents the compaction of these particles when pressure is applied. The packing of the quartz microparticles, even under pressure creates voids that allow the far smaller *MOG* particles to accommodate within them and withstand the pressure without affecting the fluorescence emission. In addition, composite material exhibits chemical stability comparable to that of the pristine (non-silica containing) metallogel. The preliminary visual inspection of the single component MOG-SiO_2 composites provided the expected red, green, and blue emissions for *Zr-BTC-TCPP-*SiO_2, *Zr-BTC-NDC-*SiO_2 and *Zr-BTC-FL-*SiO_2, respectively (Figure 3b). Since, unless neat MOG, MOG-SiO_2 composites exhibited a reproducible fluorescence response, a fine-tuning of the fluorophore concentrations in *Zr-BTC-NDC-FL-TCPP-*SiO_2 was performed until the combination of the three emissions provided a white emission (Figure 3b). The best results were obtained using 1.66 mmol $ZrCl_4$, 2.716 mmol H_3BTC, 0.030 mmol HFL, 0.282 mmol H_2NDC and a surprisingly low value of only $2.5 \cdot 10^{-3}$ mmol H_4TCPP due to its very effective self-quenching capacity. The immersion of the composites in different solvents produced fluorescence emission colour changes related to the non-equivalent changes in the response of each fluorophore, that were appreciable visually (Figure 3b) and registered in the spectra below discussed. The possible leaching of the fluorescence active molecules and zirconium atoms, when exposed to these solvents and also to different molecules dissolved in water, was checked by fluorescence analysis and elemental analysis of the washing liquid. The results showed that leaching was negligible, and the anchorage of the active molecules is strong enough for their involvement in sensing applications. Emission colour changes were also observed in the presence of different organic molecules (benzyl alcohol, caffeine, fructose, glucose, imidazole, phenol and urea) dissolved in water when the samples were immersed in these solutions. Despite in most cases the *MOG-*SiO_2 remained stable allowing its reutilization, it was noticed that carboxylic molecules or other molecules with functional groups that can strongly coordinate to the

Preprints.org (www.preprints.org) | NOT PEER-REVIEWED | Posted: 7 November 2024 doi:10.20944/preprints202411.0531.v1

zirconium metal center create a significant leaching of the fluorophore molecules (mainly fluorescein as deduced from resulting green/yellow fluorescence observed in the mother liquid).

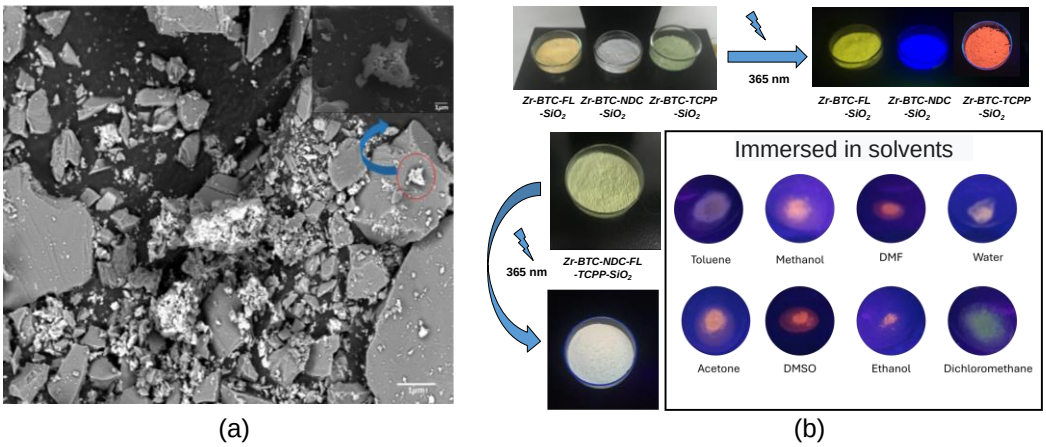

Figure 3. (a) SEM micrographs at 1000x magnification of *Zr-BTC-FL-SiO₂* as a representative case of *MOG-SiO₂* composites. Upper right inset: selected area 25000x magnification showing details of the MOG. (b) Images of the *MOG-SiO₂* composites. Top left: colour of the composites containing a single fluorophore irradiated by daylight. Top right: fluorescence emission of the composites containing a single fluorophore irradiated at 365 nm. Bottom left: *Zr-BTC-NDC-FL-TCPP-SiO₂* under daylight and irradiated at 365 nm (notice the white colour emerging from the combination of the three elemental colours). Bottom right: colours emerging from the combination of the fluorescence emissions of *Zr-BTC-NDC-FL-TCPP-SiO₂* when immersed in different solvents and excited at 325 nm.

The three emission maxima present in the multifluorophore *Zr-BTC-NDC-FL-TCPP-SiO₂* sample provides the opportunity to use their fluorescence spectra for the univocal identification of chemical species based on a stimuli-response interaction with the MOG matrix. The eye sensitivity is greater for green and lower for blue and red colours [28], which means that although perceiving through our eyes a white emission, it does not mean the intensity of the emission from the three fluorophores is equal. However, as our goal is to develop a quantitative sensoric system, we must try to get these emissions intensities as close as possible to achieve similar sensitivity for each fluorophore. In this sense, the excitation spectrum for each fluorophore was measured and the excitation wavelength was fixed at 325 nm, the value in which three fluorophore emissions are closer (Figure 4).

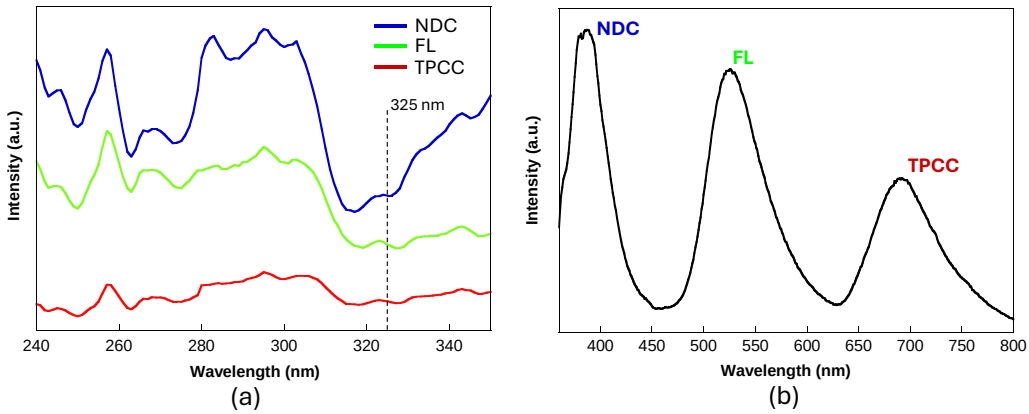

Figure 4. (a) Excitation spectra of the three fluorophores employed. (b) Emission spectra of *Zr-BTC-NDC-FL-TCPP-SiO₂* excited at 325 nm.

The quantitative analysis of intensity of each fluorescence emission could in principle provide a sensing opportunity for the solvents and for the analytes dissolved in water if the mass concentration of the analyte is kept fixed (0.1 mg/mL). However, as the fluorescence signal's intensity depends greatly on the excitation intensity of the UV source and the amount of sample, among other

 doi:10.20944/preprints202411.0531.v1

parameters, a different approach was used employing relative intensities. As we have three fluorophores incorporated simultaneously, their main emissions NDC (I_1; 387 nm), FL (I_2; 525 nm) and TCPP (I_3; 690 nm) and three relative intensity values I_1/I_2, I_1/I_3 and I_2/I_3 can be employed for the analysis. These measurements (Figure 5) must be performed while the solid sample is immersed in the solvent or aqueous solution which implies a specific setup for the experiment, A quartz cuvette originally designed for liquid measurement was used. The *Zr-BTC-NDC-FL-TCPP-SiO₂* composite (0.1 g) immersed in the solvent or aqueous solution (10 mL) was transferred to this cuvette. The particles were forced to deposit on the quartz window using a centrifuge. The whole procedure was repeated three times for every solvent or analyte to verify data's reproducibility (Tables 1, S1 and S2). A detailed description of the procedure can be found in the materials and methods section and in a video provided as supplementary material. Depicting these relative intensity values in a 3D diagram the solvents and analytes can be easily distinguished (Figure 6).

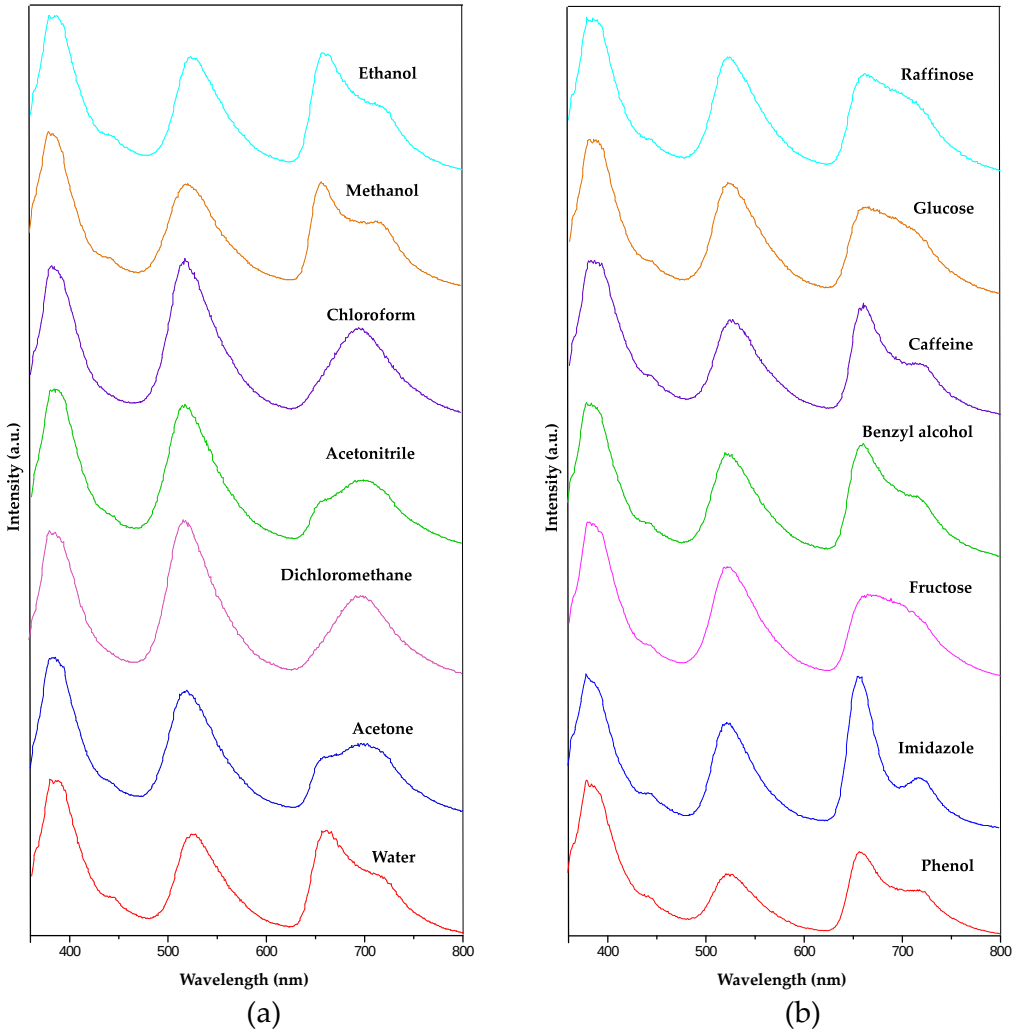

Figure 5. Fluorescence emission of *Zr-BTC-NDC-FL-TCPP-SiO₂* when immersed in different solvents (a) and molecules dissolved in water, 0.1 g/mL (b).

Table 1. Fluorescence intensity values (a.u.) for *Zr-BTC-NDC-FL-TCPP-SiO₂* when immersed in different solvents and aqueous solutions of different molecules (0.1 g/mL). The reported values correspond to the mean value and standard deviation from three measurements.

Solvents	I_1 (NDC)	I_2 (FL)	I_3 (TCPP)	I_1/I_2	I_1/I_3	I_2/I_3
Water	513(2)	337(4)	344(10)	1.52(2)	1.49(4)	0.97(3)

Preprints.org (www.preprints.org) | NOT PEER-REVIEWED | Posted: 7 November 2024 doi:10.20944/preprints202411.0531.v1

Acetone	553(9)	437(4)	257(6)	1.27(2)	2.15(6)	1.70(4)
Methanol	624(4)	431(12)	431(21)	1.45(4)	1.45(7)	1.00(6)
Ethanol	511(4)	377(10)	396(14)	1.36(4)	1.29(5)	0.95(4)
Acetonitrile	583(13)	521(2)	245(6)	1.12(3)	2.38(8)	2.13(5)
Dichloromethane	405(5)	437(12)	228(2)	0.93(3)	1.78(1)	1.92(3)
Aqueous solutions	**I_1 (NDC)**	**I_2 (FL)**	**I_3 (TCPP)**	**I_1/I_2**	**I_1/I_3**	**I_2/I_3**
Glucose	514(8)	372(13)	302(13)	1.38(4)	1.70(8)	1.23(6)
Urea	520(2)	364(7)	343(22)	1.43(3)	1.52(10)	1.06(7)
Fructose	516(6)	379(8)	283(7)	1.36(3)	1.82(5)	1.34(4)
Imidazole	521(7)	369(9)	512(14)	1.41(4)	1.02(3)	0.72(3)
Benzyl alcohol	507(5)	358(9)	385(9)	1.42(4)	1.32(3)	0.93(3)
Caffeine	477(9)	314(27)	337(9)	1.52(14)	1.42(17	0.93(14)
Phenol	434(6)	180(2)	239(2)	2.41(4)	1.81(3)	0.75(1)

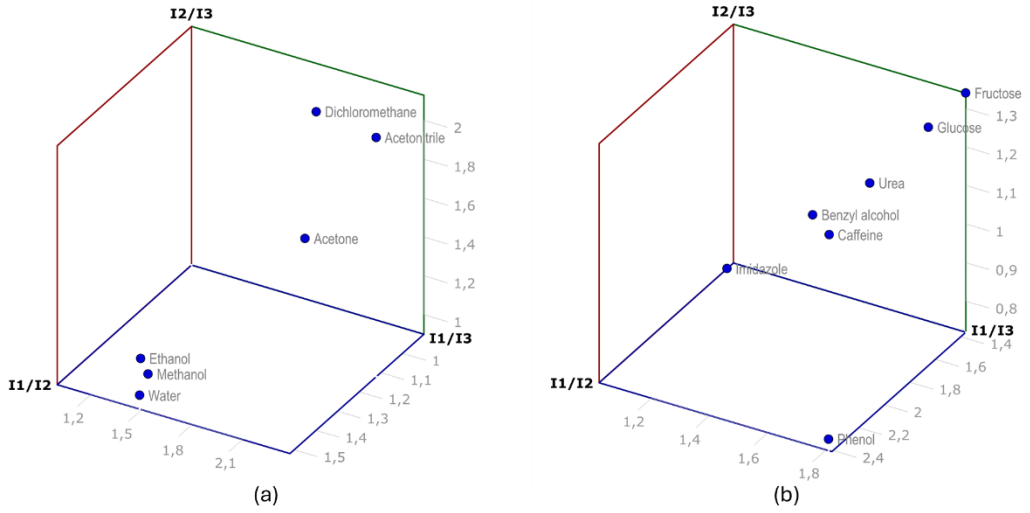

Figure 5. Depiction of the relative intensity fluorescence emission values in a three-dimensional map for the solvents (a) and molecules dissolved in water (b). I_1, I_2, and I_3 correspond to the intensity at the maximum of the peak corresponding to NDC, FL and TCPP fluorophores, respectively.

A comparable method could be developed using samples that contain a single fluorophore[7,29,30], but the results for different solvents/molecules would spread in just one dimension providing less differentiated results or less specificity in the identification. Another option would be to employ three sets of samples with just one fluorophore in each one, but strict control on the sample amount and measurement setup would be required.

3. Conclusions

Zirconium polycarboxylate gels functionalized with multiple fluorophores were successfully developed for advanced fluorescence sensing applications. By incorporating fluorescein, naphthalene-2,6-dicarboxylic acid and 4,4',4'',4'''-(porphine-5,10,15,20-tetrayl)tetrakisbenzoic acid into a robust zirconium-based gel matrix, the material demonstrated selective and tunable fluorescence responses to different solvents and analytes. The incorporation of quartz microcrystals improved mechanical stability, enabling reproducible fluorescence measurements. The ability of the composite to detect and differentiate analytes in aqueous solutions highlights its potential for chemical sensing applications. This research provides a promising basis for the development of stable, versatile fluorescent sensors in environmental and analytical chemistry [31–33].

4. Materials and Methods

 doi:10.20944/preprints202411.0531.v1

Zirconium(IV) chloride, benzene-1,3,5-tricarboxylic acid (trimesic acid, H_3BTC), fluorescent molecules and solvents were purchased from Sigma-Aldrich and used without any prior purification. Additionally, silicon dioxide particles (Sigma-Aldrich: sand, white quartz powder, >230 mesh) were employed for the formation of the gel-quartz composites.

4.1. Synthesis of MOGs and MOG-SiO_2 Composites Functionalized with Fluorophore Molecules

Following a previously described procedure [9], $ZrCl_4$ (0.389 g, 1.66 mmol) dissolved in a methanolic/aqueous solution (4.8 mL and 0.2 mL, respectively) was added to trimesic acid (0.231 g, 1.11 mmol) dissolved in 8 mL methanol, resulting in a Zr:COOH molar ratio of 1:2 as present in the $[Zr_6O_4(OH)_4(OOCR)_{12}]$ SBU [34]. The final solution was sonicated on an ultrasound bath (P selecta Ultrasons-H) at room temperature until the solution turned from transparent to translucent (aprox. 1-2 min). The vial inversion probe corroborated the correct gelation of the reaction mixture. In the case of MOGs compounds with the fluorescence molecules, the corresponding fluorophore molecule was added in the trimesic acid solution, maintaining the Zr:COOH groups molar ratio of 1:2 (Table 2). The same conditions but adding micrometic powder quartz crystals (10 g, 170 mmol) and applying vigorous stirring for 24h instead of sonication were employed to obtain the MOG-SiO_2 composites. The obtained samples were thoroughly washed in water (12h replacing the water every 2h) to remove all the remnants of the unreacted reagents. Later the sample was collected by filtration, washed with ethanol and dried under room conditions. Samples were stored protected from the light.

Table 2. Sample coding and reagent amounts employed for the synthesis MOGs.

Code	H_3BTC (mmol)	HFL (mmol)	H_2NDC (mmol)	H_4TCPP (mmol)
Zr-BTC-FL	1.090	0.050	-	-
Zr-BTC-NDC	0.560	-	0.820	-
Zr-BTC-TCPP	1.105	-	-	0.001
Zr-BTC-NDC-FL-TCPP	1.069	0.050	0.030	0.001

4.2. Fluorescence Measurements

The fluorescence measurements were performed on an Agilent Technologies Cary eclipse Fluorescence Spectrophotometer. The MOG measurements were performed placing the gels in sampled holder for solids in which the sample is hold between a high performance Quartz Glass and a presser. The observed fluorescence highly depends on the pressure applied. The measurements on the composite Zr-BTC-NDC-FL-TCPP-SiO_2 were completed using Hellma® micro absorption cuvettes (High Performance Quartz Glass, spectral range 200-2,500 nm, pathlength 10 mm, chamber volume 700 µL). The measurement of the fluorescence emission while immersed in the different solvents and aqueous solutions was accomplished using the following procedure. 0.1 g of Zr-BTC-NDC-FL-TCPP-SiO_2 and 10 mL of the corresponding solvent or aqueous solutions were placed in a test tube and left for 20 minutes with gentle stirring. Later the test tube is centrifugated at 3000 rpm for 5 min on a LAN.TECHNICS centrifuge. The solid is then transferred to the Hellma® micro absorption cuvette using a Pasteur pipette ensuring that the composite particles are always immersed in the liquid by filling the curvette with these solvents or aqueous solutions. The cuvette is now placed in the centrifuge with its glass window aligned with the rotation axis. The centrifuge force makes the particles of the composite-sample to pile up in the outer quartz window. The cuvette is now placed in the fluorescence spectrometer and the measurement takes place. The whole procedure was repeated three times for every reported data to verify the reproducibility of the measurements (Tables S1 and S2). All the measuring procedure is detailed in a video provided as supplementary material

4.3. Physical Measurements

Scanning electron microscopy (SEM) measurements of the samples were conducted on an FEG-SEM JEOL 7000F scanning electron microscope in secondary electron (SE) and backscattered electron (BSE) modes, at magnifications between ×1k and ×10k, using an accelerating of 20 kV, a current

 doi:10.20944/preprints202411.0531.v1

intensity of 1 nA, and an approximate working distance of 10 mm. Elemental mapping during SEM analysis was performed by energy-dispersive X-ray spectroscopy (EDX) using an Oxford INCA X-sight Series Si(Li) pentaFET detector. Prior to SEM measurements, the samples were attached to the sample holder using double-sided adhesive carbon tape and coated with a carbon layer by sputtering using the Q150T sample preparation kit (Quorum Technologies Ltd). Fourier-transform infrared (FTIR, KBr pellets) spectra of the samples were recorded at a resolution of 4 cm^{-1} in the 4000–500 cm^{-1} region using a FTIR 8400S Shimadzu spectrometer. The KBr pellets of the compounds have been prepared at a concentration of 2-3% using spectroscopic grade KBr (Sigma-Aldrich) that has been previously dried at 130ºC. Thermal analysis (TGA) was performed on a METTLER TOLEDO TGA/SDTA851 thermal analyzer in synthetic air (80% N_2, 20% O_2) flux of 50 $cm^3 \cdot min^{-1}$, from room temperature to 800 °C with heating rate of 5 °C min^{-1}, using alumina crucibles, and a sample size of about 10–20 mg per run.

Supplementary Materials: The following supporting information can be downloaded at the website of this paper posted on Preprints.org, FTIR spectroscopy, thermogravimetric analysis, scanning electron microscopy, additional fluorescence measurements. Video detailing the fluorescence measurement for composite Zr-BTC-NDC-FL-TCPP-SiO_2 when immersed in a liquid.

Author Contributions: The manuscript was written through contributions of all authors that given approval to the final version. †The author JPC performed the synthetic procedures. JPC, JC. and ML performed the fluorescence experiments. OC, AL, GB, and SPY designed the experiments and contributed to formal analysis. JPC, OC and AL wrote, reviewed and edited the manuscript and the supplementary information. OC and AL contributed to funding acquisition, projects administration and supervision.

Funding: This research was funded by Basque Government, grant number IT1722-22, IT1755-22 and ELKARTEK KK-2022/00032; Spanish Ministry of Science and Innovation, grant numbers TED2021-129810B-C22 and TED2021-132440B-I00 financed by MCIN/AEI/10.13039/501100011033 and by European Union NextGenerationEU/PRTR, and PID2022-138968NB-C22 project funded by MCIN/AEI/10.13039/501100011033; Red Guipuzcoana de Ciencia, Tecnología e Innovación (FA385/2023, DG23/16); and Junta de Andalucía (P21_00386). JPC thanks for the grant doctoral Research Staff Improvement (POS_2023_1_0059) funded by Basque Government.

Acknowledgments: In this section, you can acknowledge any support given which is not covered by the author contribution or funding sections. This may include administrative and technical support, or donations in kind (e.g., materials used for experiments).

Conflicts of Interest: The authors declare no conflicts of interest.

References

1. Cao, W.; Lin, Z.; Zheng, D.; Zhang, J.; Heng, W.; Wei, Y.; Gao, Y.; Qian, S. Metal-Organic Gels: Recent Advances in Their Classification, Characterization, and Application in the Pharmaceutical Field. *J. Mater. Chem. B* **2023**, *11*, 10566–10594.
2. Cavka, J.H.; Jakobsen, S.; Olsbye, U.; Guillou, N.; Lamberti, C.; Bordiga, S.; Lillerud, K.P. A New Zirconium Inorganic Building Brick Forming Metal Organic Frameworks with Exceptional Stability. *J. Am. Chem. Soc.* **2008**, *130*, 13850–13851.
3. Chattopadhyay, K.; Mandal, M.; Maiti, D.K. A Review on Zirconium-Based Metal-Organic Frameworks: Synthetic Approaches and Biomedical Applications. *Mater. Adv. s* **2023**, *5*, 51–67.
4. Angulo-Ibáñez, A.; Beobide, G.; Castillo, O.; Luque, A.; Pérez-Yáñez, S.; Vallejo-Sánchez, D. Aerogels of 1D Coordination Polymers: From a Non-Porous Metal-Organic Crystal Structure to a Highly Porous Material. *Polymers* **2016**, *8*, 1–12.
5. Zhao, F.; Yang, W.; Han, Y.; Luo, X.; Tang, W.; Yue, T.; Li, Z. A Straightforward Strategy to Synthesize Supramolecular Amorphous Zirconium Metal-Organic Gel for Efficient Pb(II) Removal. *Chem. Eng. J.* **2021**, *407*, 126744.
6. Shaiful Bahari, A.M.; Othman, S.Z.; Mohamad Fadli, M.F.; Zulkifli, M.Z.A.; Biyamin, S.A.; Islam, M.A.; Aspanut, Z.; Amin, N.; Misran, H. Facile Synthesis of Zr-Based Metal-Organic Gel (Zr-MOG) Using "Green" Sol-Gel Approach. *Surf. Interfaces* **2021**, *27*, 101469.
7. Liu, W.S.; Yang, Y.; Zhong, Q.K.; Xu, Z.P.; Zhang, J.Z.; Yao, B. Ben; Lian, X.; Niu, H.L. Zr^{4+}-Based Metal Organic Gel as a Fluorescent "Turn on-off" Sensing Platform for the Selective Detection and Adsorption of CrO_4^{2-}. *Mater. Chem. Front.* **2021**, *5*, 1932–1941.
8. Wang, J.; Xiao, X.; Lu, Y.; Wang, Y.; Chen, C.; Pang, H. Zirconium-Based Materials for Electrochemical Energy Storage. *ChemElectroChem* **2019**, *6*, 1949–1968.

9. Tan, C.; Xu, Z.; Zhang, L.; Lei, M.; Lei, J.; Duan, T.; Liu, W. Introducing Zirconium Organic Gels for Efficient Radioiodine Gas Removal. *Inorg. Chem.* **2022**, *61*, 4818–4824.
10. Santos-Lorenzo, J.; San José-Velado, R.; Albo, J.; Beobide, G.; Castaño, P.; Castillo, O.; Luque, A.; Pérez-Yáñez, S. A Straightforward Route to Obtain Zirconium Based Metal-Organic Gels. *Micropor. Mesopor. Mat* **2019**, *284*, 128–132.
11. Li, Y.; Young, D.J.; Loh, X.J. Fluorescent Gels: A Review of Synthesis, Properties, Applications and Challenges. *Mater. Chem. Front.* **2019**, *3*, 1489–1502.
12. Sun, S.; Wei, C.; Xiao, Y.; Li, G.; Zhang, J. Zirconium-Based Metal-Organic Framework Gels for Selective Luminescence Sensing. *RSC Adv.* **2020**, *10*, 44912–44919.
13. Liu, M.; Xia, S.; Liu, Z.; Ma, T.; Liu, Z.; Li, Y.; Zou, D. Luminescent Porous Metal-Organic Gels for Efficient Adsorption and Sensitive Detection of Chlortetracycline Hydrochloride Assisted by Smartphones and a Test Paper-Based Analytical Device. *Inorg. Chem. Front.* **2022**, *9*, 1722–1734.
14. Aliev, S.B.; Gurskiy, S.I.; Zakharov, V.N.; Kustov, L. Synthesis of Novel Nanoporous Metal-Organic Gels with Tunable Porosity and Sensing of Aromatic Compounds. *Micropor. and Mesopor. Mat.* **2018**, *264*, 112–117.
15. Sun, S.; Wei, C.; Xiao, Y.; Li, G.; Zhang, J. Zirconium-Based Metal-Organic Framework Gels for Selective Luminescence Sensing. *RSC Adv.* **2020**, *10*, 44912–44919.
16. Zou, C.; Xie, M.H.; Kong, G.Q.; Wu, C. De Five Porphyrin-Core-Dependent Metal-Organic Frameworks and Framework-Dependent Fluorescent Properties. *CrystEngComm* **2012**, *14*, 4850–4856.
17. Li, Y.; Chai, B.L.; Xu, H.; Zheng, T.F.; Chen, J.L.; Liu, S.J.; Wen, H.R. Temperature- and Solvent-Induced Reversible Single-Crystal-to-Single-Crystal Transformations of Tb^{III}-Based MOFs with Excellent Stabilities and Fluorescence Sensing Properties toward Drug Molecules. *Inorg. Chem. Front.* **2022**, *9*, 1504–1513.
18. Hou, J.; Sapnik, A.F.; Bennett, T.D. Metal-Organic Framework Gels and Monoliths. *Chem. Sci.* **2020**, *11*, 310–323.
19. Shaiful Bahari, A.M.; Othman, S.Z.; Mohamad Fadli, M.F.; Zulkifli, M.Z.A.; Biyamin, S.A.; Islam, M.A.; Aspanut, Z.; Amin, N.; Misran, H. Facile Synthesis of Zr-Based Metal-Organic Gel (Zr-MOG) Using "Green" Sol-Gel Approach. *Surfaces and Interfaces* **2021**, *27*, 101469, doi:10.1016/j.surfin.2021.101469.
20. Massimi, S.E.; Metzger, K.E.; McGuirk, C.M.; Trewyn, B.G. Best Practices in the Characterization of MOF@MSN Composites. *Inorg. Chem.* **2022**, *61*, 4219–4234
21. Tella, A.C.; Owalude, S.O.; Omotoso, M.F.; Olatunji, S.J.; Ogunlaja, A.S.; Alimi, L.O.; Popoola, O.K.; Bourne, S.A. Synthesis, Crystal Structures and Luminescence Properties of New Multi-Component Co-Crystals of Isostructural Co(II) and Zn(II) Complexes. *J. Mol. Struct.***2018**, *1157*, 450–456.
22. Gangu, K.K.; Dadhich, A.S.; Mukkamala, S.B. Synthesis, Crystal Structure and Fluorescent Properties of Two Metal-Organic Frameworks Constructed from Cd(II) and 2,6-Naphthalene Dicarboxylic Acid. *Inorg. Nano-Met. Chem.* **2017**, *47*, 313–319.
23. Ding, Y.; Pan, L.; Li, S.; He, H.; Zhang, D.; Hu, X.; Zhang, R.; Wang, Y.; Zhai, X.; Meng, Q. Fabrication and Investigation of 26NCA Films Exhibiting Tunable Blue Fluorescence Based on LVPVDM. *J. Nanomater.* **2018**, *2018*, 5426427.
24. Seybold, P.G.; Gouterman, M.; Callis, J. Calorimetric, Photometric and Lifetime Determinations of Fluorescence Yields of Fluorescein Dyes. *Photochem. and Photobiol.* **1969**, *9*, 229–242.
25. Quiroz-Segoviano, R.I.Y.; Serratos, I.N.; Rojas-González, F.; Tello-Solís, S.R.; Sosa-Fonseca, R.; Medina-Juárez, O.; Menchaca-Campos, C.; García-Sánchez, M.A. On Tuning the Fluorescence Emission of Porphyrin Free Bases Bonded to the Pore Walls of Organo-Modified Silica. *Molecules* **2014**, *19*, 2261–2285.
26. Makarska-Bialokoz, M. Spectroscopic Study of Porphyrin-Caffeine Interactions. *J. Fluoresc.* **2012**, *22*, 1521–1530.
27. Rajasree, S.S.; Li, X.; Deria, P. Physical Properties of Porphyrin-Based Crystalline Metal–organic Frameworks. *Commun. Chem.* **2021**, *4*, 1–14.
28. Thorseth, A. Photometry — The CIE System of Physical Photometry. *ISO/CIE* **2023**, 23539.
29. Qi, H.; Zhang, T.; Jing, C.; Zhang, Z.; Chen, Y.; Chen, Y.; Deng, Q.; Wang, S. Metal-Organic Gel as a Fluorescence Sensing Platform to Trace Copper(II). *Anal. Methods* **2022**, *14*.
30. Feng, X.; Zeng, L.; Zou, D.; Zhang, Z.; Zhong, G.; Peng, S.; Liu, L.; Chen, L.; Zhang, J. Trace-Doped Metal-Organic Gels with Remarkably Enhanced Luminescence. *RSC Adv.* **2017**, *7*, 37194–37199.
31. Zhang, X.Y.; Yang, Y.S.; Wang, W.; Jiao, Q.C.; Zhu, H.L. Fluorescent Sensors for the Detection of Hydrazine in Environmental and Biological Systems: Recent Advances and Future Prospects. *Coord. Chem. Rev.* **2020**, *417*, 213367.
32. New, A.A.; Bowyer, E.J. Fluorescent Platforms for Environmental Sensing. In *Fluorescent Chemosensors*; James, L.W.A.C.S.X.-P.H.T.D., Ed.; Royal Society of Chemistry, 2023; pp. 378–405 ISBN 978-1-83916-386-9.
33. Fakayode, S.O.; Lisse, C.; Medawala, W.; Brady, P.N.; Bwambok, D.K.; Anum, D.; Alonge, T.; Taylor, M.E.; Baker, G.A.; Mehari, T.F.; et al. Fluorescent Chemical Sensors: Applications in Analytical, Environmental, Forensic, Pharmaceutical, Biological, and Biomedical Sample Measurement, and Clinical Diagnosis. *Appl. Spectrosc. Rev.* **2024**, *59*, 1–89.

 doi:10.20944/preprints202411.0531.v1

34. Nam, D.; Kim, J.; Choe, W. Evolution of Zr Nodes in Metal–Organic Frameworks. *Trends Chem.* **2023**, *5*, 339–352.